The Conserved Tyrosine Residues 401 and 1044 in ATP Sites of Human P-Glycoprotein Are Critical for ATP Binding and Hydrolysis: Evidence for a Conserved Subdomain, the A-Loop in the ATP-Binding Cassette†

In-Wha Kim,‡,§ Xiang-Hong Peng,‡,§,|| Zuben E. Sauna,‡ Peter C. FitzGerald,⊥ Di Xia,‡ Marianna Müller,‡,@ Krishnamachary Nandigama,‡ and Suresh V. Ambudkar*,‡

Laboratory of Cell Biology and Genome Analysis Unit, Center for Cancer Research, National Cancer Institute, National Institutes of Health, Bethesda, Maryland 20892

Received February 14, 2006; Revised Manuscript Received April 21, 2006

ABSTRACT: Each nucleotide-binding domain (NBD) of mammalian P-glycoproteins (Pgps) and human ATP-binding cassette (ABC) B subfamily members contains a tyrosine residue ∼25 residues upstream of the Walker A domain. To assess the role of the conserved Y401 and Y1044 residues of human Pgp, we substituted these residues with F, W, C, or A either singly or together. The mutant proteins were expressed in a *Vaccinia* virus-based transient expression system as well as in baculovirus-infected HighFive insect cells. The Y401F, Y401W, Y1044F, Y1044W, or Y401F/Y1004F mutants transported fluorescent substrates similar to the wild-type protein. On the other hand, Y401L and Y401C exhibited partial (30−50%) function, and transport was completely abolished in Y401A, Y1044A, and Y401A/Y1044A mutant Pgps. Similarly, in Y401A, Y1044A, and Y401A/Y1044A mutants, TNP−ATP binding, vanadate-induced trapping of nucleotide, and ATP hydrolysis were completely abolished. Thus, an aromatic residue upstream of the Walker A motif in ABC transporters is critical for binding of ATP. Additionally, the crystal structures of several NBDs in the nucleotide-bound form, data mining, and alignment of 18 514 ABC domains with the consensus conserved sequence in a database of all nonredundant proteins indicate that an aromatic residue is highly conserved in ∼85% of ABC proteins. Although the role of this aromatic residue has previously been studied in a few ABC proteins, we provide evidence for a near-universal structural and functional role for this residue and recognize its presence as a conserved subdomain ∼25 amino acids upstream of the Walker A motif that is critical for ATP binding. We named this subdomain the "A-loop" (aromatic residue interacting with the adenine ring of ATP).

P-Glycoprotein (Pgp,[1] ABCB1), encoded by the human *MDR*1 gene, is a member of the ATP-binding cassette (ABC) transporter superfamily. Pgp is implicated in the resistance of tumors to anticancer drugs and is also known to transport several other classes of amphipathic compounds such as steroids and antiviral, antifungal, and anticardiac drugs (*1*−*3*). The functional unit of Pgp, a 150−170 kDa phosphorylated glycoprotein containing 1280 amino acids, is composed of two homologous halves, each half containing six transmembrane domains and one nucleotide-binding domain (NBD), separated by a flexible linker region (*4*−*6*). The ABC or the nucleotide-binding domain (NBD) contains several conserved motifs including the Walker A motif, the Walker B motif, the ABC signature linker region or "C" region, the D loop, the H loop, and the Q loop (*7*, *8*). Although ATP binding and hydrolysis appear to be essential for the proper functioning of Pgp, including drug transport (*9*), the exact mechanism of how the energy derived from ATP hydrolysis is used for the transport of drugs still needs to be elucidated. Understanding the role(s) of conserved amino acids in the nucleotide-binding region is an important aspect of this goal. Site-directed mutagenesis approaches have been used to study the role of several conserved residues in the NBD, including D555, D1200, E556, E1201, S532, S1177, Q475, and Q1118 (or their equivalent in mouse MDR3) (*3*). Moreover, the crystal structures of ABCs of several ABC transporters, viz. bacterial HisP (*10*), MJ0796 (*11*), MJ1267 (*12*), MalK (*13*, *14*), GlcV (*15*), MsbA (*16*) mouse and human cystic fibrosis transmembrane regulator (CFTR) NBD1 (*17*, *18*), and human Tap1 (*19*), suggest that a conserved tyrosine or another aromatic residue interacts with the adenine ring of the nucleotide. A recently determined structure of a bacterial ABC protein, RLI (an RNase-L inhibitor), also shows that the adenine ring of the ADP molecule was situated in a

† This research was supported by the Intramural Research Program of the National Institutes of Health, National Cancer Institute, Center for Cancer Research.

* To whom correspondence should be addressed. Phone: (301) 402-4178. Fax: (301) 435-8188. E-mail: ambudkar@helix.nih.gov.

‡ Laboratory of Cell Biology.

§ These authors contributed equally to this work.

|| Present address: Department of Surgery, Winship Cancer Institute, Emory University, Atlanta, GA 30322.

⊥ Genome Analysis Unit.

@ Present address: Department of Molecular Cell Biology, National Medical Center, Budapest, Hungary.

[1] Abbreviations: ABC, ATP-binding cassette; BeF_x, beryllium fluoride; DTT, dithiothreitol; IAAP, [^{125}I]iodoarylazidoprazosin; MDR, multidrug resistance; NBD, nucleotide-binding domain; PAGE, polyacrylamide gel electrophoresis; Pgp, P-glycoprotein; TNP-ATP, 2′-*O*-(trinitrophenyl)adenosine 5′-triphosphate; Vi, sodium orthovanadate.

10.1021/bi060308o
Published on Web 05/26/2006

shallow aromatic/hydrophobic groove, the "Y loop" formed by a tyrosine residue (*20*). These structures indicate that the aromatic residue interacts with the adenine ring of ATP by $\pi-\pi$ stacking, hydrogen bonding, or van der Waals interaction (*14*, *21*). It was recently suggested that hydrogen bonding interaction is involved at the Watson−Crick edge between the central adenylate and the Y residue (*22*).

It was reported that the mutation of Tyr16 to a serine residue in the HisP subunit of histidine permease abolished the binding of ATP and its transport function (*23*). In contrast, the mutation of residues F429, F430, F433, and F1232 (the residue corresponding to F430 in NBD2 of CFTR is Y1219 and not F1232) to Cys in human CFTR did not affect the chloride channel function (*24*). Similarly, a recent study demonstrated that in MRP1, substitution of W653 in NBD1 or Y1302 in NBD2 with C resulted in a decrease in the affinity for ATP and an increase in LTC4 transport activity (*25*). It has also been shown that Tyr398 and Tyr1041 in hamster Pgp were cross-linked with 8-azido[α-^{32}P]ADP during vanadate (Vi)-induced nucleotide trapping (*26*), suggesting that these Tyr residues might be involved in ATP binding (*27*). These studies raise some important questions. Is an interaction between an aromatic residue and the adenine ring of ATP universal to all ABC proteins? Are some aromatic residues preferred over others? What is the structural and spatial relationship, if any, between the aromatic residue and other conserved domains of the ABC? Is the aromatic residue itself an integral part of the consensus ABC domain?

The tyrosine residues at positions 401 and 1044 in the N- and C-NBDs, respectively, of human Pgp are equivalent to the aromatic residues discussed above. The purpose of this study was to determine whether the Y401 and Y1044 residues in NBD1 and NBD2 play a role in ATP binding and/or hydrolysis by human Pgp and whether this residue represents a conserved subdomain, which is present in a majority of ABC transporters. Systematic biochemical characterization of these residues in Pgp by a mutational study demonstrates that only aromatic residues (Y, W, and F) at this position allow full retention of function, whereas residues such as L or C support only partial (30−50%) activity. Moreover, an atomic model of the NBD1−NBD2 dimer of Pgp based on the crystal structure of the E171Q mutant NBD of MJ0796 (*28*) shows that this tyrosine residue stacks against the adenine ring of ATP. In addition, large-scale data mining, sequence alignment, and analysis of nucleotide-bound structures of several NBDs indicate the presence of an aromatic residue at a position 25 amino acids upstream of the Walker A motif in a majority of ABC transporters. On the basis of these multiple approaches, we provide evidence for a near-universal structural and functional role for this residue in NBDs of ABC proteins. We propose that this conserved residue should be considered an integral part of the ABC domain. To emphasize its interaction with the adenine ring of ATP, we named this subdomain the "A-loop" (aromatic residue interacting with the adenine ring of ATP).

EXPERIMENTAL PROCEDURES

Chemicals. Dulbecco's modified Eagle's medium (DMEM), Iscove's modified Dulbecco's medium (IMDM), L-glutamine, and penicillin/streptomycin were obtained from Life Technologies (Gaithersburg, MD). The Lipofectin reagent kit and PCR primers were purchased from Invitrogen (Carlsbad, CA), and FBS was supplied by HyClone (Logan, UT). Restriction enzymes and T4 DNA ligase were from New England Biolabs (Beverly, MA). The Expand High Fidelity PCR system was from Boehringer Mannheim (Roche Diagnostics Corp., Indianapolis, IN). A recombinant *Vaccinia* virus encoding bacteriophage T7 RNA polymerase (vTF7-3) was obtained from B. Moss (National Institute of Allergy and Infectious Disease, National Institutes of Health). Pgp-specific monoclonal antibody C219 was obtained from Fujirebio Diagnostics Inc. (Malvern, PA), and human Pgp-specific monoclonal antibody MRK16 was purchased from Kyowa Medex Co., Ltd. (Tokyo, Japan). FITC-conjugated anti-mouse IgG_{2a} secondary antibody was obtained from PharMingen (San Diego, CA). ECL reagents were obtained from Amersham Pharmacia Biotech, Inc. (Piscataway, NJ). Calcein-AM and TNP-ATP were purchased from Molecular Probes, Inc. (Eugene, OR). Cyclosporine A was purchased from Calbiochem (San Diego, CA). [^{125}I]Iodoarylazidoprazosin (IAAP, 2200 Ci/mmol) and [α-^{32}P]ATP (3000 Ci/mmol) were obtained from PerkinElmer Life Sciences (Boston, MA). 8-Azido[α-^{32}P]ATP (15−20 Ci/mmol), 8-azido-[γ-^{32}P]ATP (15−20 Ci/mmol), and 8-azidoATP were purchased from Affinity Labeling Technologies, Inc. (Lexington, KY). All other chemicals were obtained from Sigma Chemical Co. (St. Louis, MO).

Identification and Alignment of Protein Regions Containing Nucleotide-Binding Domains for ABC Transport Proteins. RPS-BLAST was used to search the nonredundant protein database (February 12, 2005) for matches to the pattern characteristic of ABC transporters (PSSM entry 5341, cd00267). This pattern consists of distinct motifs for the ATP binding site, ABC transporter signature motif, Walker A−P-loop, Walker B, D-loop, Q-loop, and H-loop−switch region (see http://www.ncbi.nlm.nih.gov/Structure/cdd/cddsrv.cgi?uid=cd00267). Matched regions with an *e* value of $\leq 1e^{-10}$ and spanning the region corresponding to the position from ~25−30 residues upstream of the Walker A motif to ~175 residues downstream of it (ATP binding motif) in the consensus pattern were combined into a multiple alignment, based on the RPS-BLAST alignments of the individual sequences to the consensus motif. The frequency of occurrence of each residue at the position corresponding to 25 residues upstream of the Walker A motif in the consensus was determined for (a) the whole data set and (b) the subset of proteins identified as being eukaryotic in origin. Additionally, the presence of W, F, or Y residues within two positions of the position 25 residues upstream of the Walker A motif was also scored. As described above, RPS-BLAST was used to identify and align the signature regions of the 87 members (48 distinct genes and isoforms) of the human ABC transporter protein family [see a recent review by Dean and Annilo (*29*)]. Where appropriate, Clustal W (*30*) was used to generate multiple-sequence alignment of various subgroupings of this large family.

Vaccinia Virus Expression Vector Constructs. Site-directed mutations were constructed by a sequence overlap PCR gene fusion technique using an Expand High Fidelity PCR kit and cloned into pTM1-*MDR*1-His6 (wild type) as the expression vector template as described previously (*31*, *32*). The DNA sequence of all constructs was verified in both directions by

automated sequencing with the PRISM Big Dye Terminator Sequencing Kit (PerkinElmer Corp., Norwalk, CT).

Cell Surface Expression of Wild-Type and Mutant Pgps and Drug Accumulation/Efflux Assays by Flow Cytometry. HeLa cells were infected with a recombinant *Vaccinia* virus encoding bacteriophage T7 RNA polymerase (vTF7-3) and transfected with wild-type or mutant plasmids, pTM1-*MDR*1-His6. Sixteen to twenty hours post-infection/transfection, cells were trypsinized and stained with the human Pgp external epitope-specific monoclonal antibody, MRK16 (*33*), and analyzed with a FACSort flow cytometer using CellQuest (Becton Dickson, San Jose, CA) as described previously (*31*, *32*). Fluorescent drug accumulation/efflux assays were performed in infected−transfected HeLa cells using a flow cytometer. The calcein accumulation assay was performed with 0.5 μM calcein-AM; 300000−500000 cells were incubated in 4 mL of IMDM with 5% FBS at 37 °C for 10 min, and the pelleted cells were analyzed by FACSort as described previously (*32*, *34*). For quantitation of the transport activity of wild-type and various mutant Pgps, FACS assays were carried out in the presence and absence of 10 mM cyclosporine A (Pgp inhibitor), and the cyclosporine A sensitive activity in terms of median fluorescence units was calculated using the histogram stat program in CellQuest. These values for wild-type (100%) and mutant Pgps are given in Table 1.

SDS−PAGE and Immunoblot Analysis. Immunoblot analysis with monoclonal antibody C219 (*35*) or polyclonal antisera PEPG-13 (*36*) was used to determine the total cellular content of the wild-type and mutant Pgps as previously described (*31*, *34*).

Preparation of Crude Membranes from HighFive Insect Cells Expressing Mutants and Wild-Type Pgp. HighFive insect cells (Invitrogen) were infected with the recombinant baculovirus carrying the wild type and Y401A, Y1044A, Y401A/Y1044A, Y401C, Y401L, and Y401W mutant human *MDR*1 cDNAs with a His_6 tag at the C-terminal end [BV-MDR1(His6)] as described previously (*37*). Crude membranes were prepared as described previously (*38*) and stored at −70 °C.

Purification and Reconstitution of Wild-Type and Mutant Pgps. The crude membranes were solubilized with octyl β-D-glucoside [1.25% (w/v)] in the presence of 20% glycerol and a lipid mixture (0.1%) (*37*, *39*). Solubilized proteins were subjected to metal affinity chromatography (Talon resin, Clontech, Palo Alto, CA) in the presence of 1.25% octyl β-D-glucoside and a 0.1% lipid mixture; 80% purified Pgp was eluted with 200 mM imidazole. Pgp in the 200 mM imidazole fraction was dialyzed to remove imidazole and NaCl at pH 8.0 (*37*, *38*) and subjected to DE-52 chromatography for further purification. The flow-through fraction was collected and concentrated (Centriprep-50, Amicon, Beverly, MA) by centrifugation at 4 °C to ∼1.0−1.5 mg/mL and stored at −70 °C. The purity of Pgp was verified by silver staining of the gel and by immunoblot analysis using monoclonal antibody C219 (*35*) and quantified by the amido black B protein estimation method as described previously (*40*). Purified Pgp in detergent solution was mixed with a sonicated lipid mixture at a 1:8−10 (protein:lipid) ratio and reconstituted into proteoliposomes via removal of the detergent by dialysis at 4 °C as described previously (*38*).

Table 1: Effect of Substitution of the Conserved Y401 and Y1044 Residues in ATP Sites on Pgp Cell Surface Expression, Transport Function, ATP Binding, Nucleotide Trapping, and Hydrolysis[a]

construct	cell surface expression[b] (%)	transport function[c] (%)	ATP binding[d] (%)	ADP−Vi trapping[e] (%)	ATP hydrolysis[f] (%)
wild-type MDR1	100	100	100	100	100
Y401W	100	100	90−95	90−95	85−90
Y401F	95−100	90−100	NT[g]	NT[g]	NT[g]
Y401C	90−95	45−55	50	<20	NT[g]
Y401L	95−100	25−30	30−35	20−25	NT[g]
Y401A	100−110	<2	<15	<2	<2
Y1044W	100	100	NT[g]	NT[g]	NT[g]
Y1044F	95−100	90−100	NT[g]	NT[g]	NT[g]
Y1044C	90−95	<2	NT[g]	NT[g]	NT[g]
Y1044A	100	<2	<5	<2	<2
Y401W/Y1044W	90−95	<2	NT[g]	NT[g]	NT[g]
Y401F/Y1044F	90−95	95−100	NT[g]	NT[g]	NT[g]
Y401C/Y1044C	100	<2	NT[g]	NT[g]	NT[g]
Y401A/Y1044A	90−95	<2	<2	<2	<2
Y401F/Y1044W	100	100	NT[g]	NT[g]	NT[g]
Y401C/Y1044W	100	<2	NT[g]	NT[g]	NT[g]
Y401A/Y1044W	100−110	<2	NT[g]	NT[g]	NT[g]
Y401W/Y1044F	100	100	NT[g]	NT[g]	NT[g]

[a] The levels of cell surface expression, transport activity, ATP binding, nucleotide trapping, and ATP hydrolysis by the wild-type protein were taken to be 100%, and these activities in mutant Pgps were expressed relative to wild-type levels. [b] Cell surface expression assessed using human Pgp-specific monoclonal antibody MRK-16 in transfected−infected HeLa cells. [c] Transport function assessed by assaying the efflux of calcein-AM (see Figure 2) in transfected−infected HeLa cells. The cyclosporine A-sensitive level of fluorescence was used to determine the efflux activity as described in Experimental Procedures. Similar results were also obtained with other substrates, including rhodamine123, Bodipy-FL-verapamil, and Bodipy-FL-vinblastine (data not shown). [d] Labeling with photoaffinity analogue 8-azido[α-^{32}P]ATP at 4 °C in baculovirus-infected HighFive insect cell membranes and TNP-ATP binding to purified proteins in proteoliposomes. [e] Vanadate-induced trapping of 8-azido[α-^{32}P]ADP at 37 °C in crude membranes of HighFive insect cells and in purified proteoliposomes containing pure protein. [f] The ATP hydrolysis assay was carried out at 37 °C using crude membranes using 5 mM ATP and a colorimetric P_i detection assay. For purified wild-type and mutant proteins reconstituted into proteoliposomes, the [α-^{32}P]ATP hydrolysis assay was used (see Figure S2 of the Supporting Information). [g] Not tested.

Binding of 8-Azido[α-^{32}P]ATP to Pgp. Crude membranes of HighFive insect cells (100−200 μg of protein) and purified and reconstituted protein (0.5−10 μg of protein) were incubated in ATPase assay buffer [50 mM MES-Tris (pH 6.8), 50 mM KCl, 5 mM sodium azide, 2 mM EGTA, 2 mM dithiothreitol, 1 mM ouabain, and 10 mM $MgCl_2$] containing 10 μM 8-azido[α-^{32}P]ATP (containing 5−10 μCi/nmol) in the dark at 4 °C for 5 min. The samples were irradiated with a UV lamp assembly (PGC Scientifics, Gaithersburg, MD) fitted with two black light (self-filtering) UV-A long wave F15T8BLB tubes (365 nm) for 10 min on ice (4 °C). Ice-cold ATP (10 mM) was added to displace excess noncovalently bound 8-azido[α-^{32}P]ATP. After SDS−PAGE on a 7% Tris-acetate NuPAGE gel, the gels were dried and exposed to Bio-Max MR film (Eastman Kodak Co.) at −70 °C for 12−24 h. The radioactivity incorporated into the Pgp band was quantified using the STORM 860 PhosphorImager system and ImageQuaNT (Molecular Dynamics, Sunnyvale, CA) and adjusted to Pgp expression levels.

Vanadate- and Beryllium Fluoride-Induced 8-Azido[α-^{32}P]-ADP Trapping in Pgp. The Pgp·Mg-8-azido[α-^{32}P]ADP·BeF_x or Pgp·Mg-8-azido[α-^{32}P]ADP·Vi pre- or posthydrolysis transition state conformation was generated as described

previously (*41*, *42*) with minor modifications. Crude membranes of HighFive insect cells (100 μg) or purified and reconstituted protein (2.5−7.5 μg) were incubated at 37 °C in ATPase assay buffer containing 50 μM 8-azido[α-^{32}P]-ATP or, in some experiments as indicated, 8-azido[α-^{32}P]-ATP (5 μCi/nmol), 300 μM Vi or 0.25 mM beryllium sulfate, and 2.5 mM sodium fluoride in the dark at 37 °C for 5 min. We stopped the reaction by adding 10 mM ice-cold ATP and placing the samples immediately on ice. The trapped nucleotides were photo-cross-linked; samples were electrophoresed, and the radioactivity incorporated in the Pgp band was quantified as described previously (*34*).

Mild Trypsin Digestion of Pgp. Crude membranes of HighFive insect cells were subjected to mild trypsin digestion to separate the N- and C-terminal half of Pgp (*41*, *43*) following nucleotide binding or trapping as described above. The labeled crude membranes containing wild-type and Y401W Pgps were treated with trypsin at a trypsin:protein ratio of 1:10 (w/w) for 5 min at 37 °C, and the reaction was terminated by adding a 5-fold excess of trypsin inhibitor. Following electrophoresis and immunoblotting with C219 or polyclonal antisera PEPG-13, the blots were exposed to fluorescent light for 12−14 h to eliminate the chemoluminescence signal. The same blot was used to obtain the ^{32}P signal by exposing it to an X-ray film at −70 °C. Colocalization of the two signals indicated that the ^{32}P-labeled radionucleotide was incorporated into both halves of wild-type and Y401W Pgps.

Photoaffinity Labeling of Wild-Type and Y401A, Y1044A, Y401A/Y1044A, and Y401W Mutant Pgps with [^{125}I]IAAP. The crude membranes of HighFive insect cells (100−200 μg) were incubated at room temperature in ATPase assay buffer (pH 6.8) with IAAP (7 nM) for 5 min under subdued light. The samples were then photo-cross-linked for 10 min at room temperature, and the subsequent steps were carried out as described above.

ATPase Assay. The Vi- or BeF_x-sensitive ATPase activity of wild-type and mutant Pgps was determined for crude membranes as the amount of P_i released measured by a colorimetric method (*44*). In addition, a more sensitive method for measurement of ATP hydrolysis by purified and reconstituted mutant Pgps was used. Hydrolysis of [α-^{32}P]-ATP was assessed by measuring the level of release of [α-^{32}P]ADP. Proteoliposomes containing purified and reconstituted Pgps (0.5−10 μg) were incubated with 0.5 mM (with 100 μCi/nmol) [α-^{32}P]ATP in the ATPase assay buffer. After incubation at 37 °C for 20 min, the reactions were terminated by adding SDS to a final concentration of 2.5% and the reaction mixture was spotted onto a polyethyleneimine cellulose TLC plate (Merck KGaA, Darmstadt, Germany) and was developed with a solution containing 1 M formic acid and 0.5 M LiCl to separate nucleotide diphosphates from triphosphates (*45*). The amount of [α-^{32}P]-ADP formed was analyzed using a STORM 860 PhosphorImager system (Molecular Dynamics). We generated a standard curve by quantifying the intensity of the signal in the PhosphorImager for the radioactivity associated with a known concentration of [α-^{32}P]ATP and used the slope to calculate the specific activity for the wild-type and mutant Pgps.

Binding of TNP-ATP to Pgp. Purified and reconstituted proteins were used for this assay. Binding of the fluorescent nucleotide analogue TNP-ATP was assessed by determining the increase in the fluorescence signal (excitation at 408 nm, emission at 540) of TNP-ATP (2.5−80 μM) associated with purified wild-type and mutant Pgps (Y401W, Y401A, Y1004A, and Y401A/Y1004A) incorporated into proteoliposomes as described previously (*42*). The fluorescence signal in the presence of a >100-fold excess ATP (10 mM) was taken to be the baseline. The concentration of TNP-ATP required for half-maximal binding was determined by measuring the signal of increasing concentrations of TNP-ATP in the presence of proteoliposomes (20−25 μg of protein/mL for the wild-type protein and Y401W mutant and 50−100 μg of protein/mL for Y401A, Y1044A, and Y401A/Y1044A mutant proteins) and in the presence and absence of 10 mM ATP. In addition, an equal volume of liposomes (prepared in the same manner as proteoliposomes but without protein) was used to the determine TNP-ATP signal in the presence and absence of 10 mM ATP.

RESULTS

Identification and Alignment of Nucleotide-Binding Domains of ABC Transporter Proteins. The search for ABC transporter domains in the set of all nonredundant proteins identified a total of 18 514 domains, of which 15 614 (84.3%) contain an aromatic residue at a position 25 residues upstream of the Walker A motif as aligned to the consensus sequences (Table S1 of the Supporting Information). This number rises to 16 312 or 88.1% if one includes the aromatic residue at a position 25 (±2) residues upstream of the Walker A motif. A search through all eukaryotic proteins identified 3024 domains, of which 2452 (81.1%) contain aromatic residues at a position 25 residues upstream of the Walker A motif. Again, this number rises to 2648 (87.6%) if one includes aromatics in the neighboring region 25 (±2) residues upstream of the Walker A motif. Moreover, aromatic amino acids in C-terminal nucleotide-binding domains are more conserved than in the N-terminus (93.4% vs 83.8%). The sequence alignment of this region of most commonly studied ABC transporters, including both full-length and half transporters and the sequence logo, shows that the tyrosine residue in NBD2 is highly conserved (see Table 1 and Figure 2 of ref *46*). On the other hand, phenylalanine or tryptophan, in addition to tyrosine, is found in NBD1 at this position.

To assess the role of conserved Y401 and Y1044 residues in the mechanism of ATP binding and hydrolysis by human Pgp, the following amino acids were introduced at these positions: A, a nonpolar nonaromatic amino acid, C, a polar nonaromatic amino acid, and F and W, nonpolar aromatic amino acids. We generated the single mutants Y401A, Y1044A, Y401C, Y1044C, Y401F, Y1044F, Y401W, Y1044W, and Y401L. We also generated the double mutants Y401A/Y1044A, Y401F/Y1044F, Y401W/Y1044W, Y401C/Y1044C, Y401A/Y1044W, Y401F/Y1044W, Y401C/Y1044W, and Y401W/Y1044F. All these mutants were initially characterized using a *Vaccinia* virus-based transient expression system, and subsequently, for detailed biochemical studies, selected mutants were expressed in baculovirus-infected HighFive insect cells and purified to homogeneity as described in Experimental Procedures. The purified wild-type and mutant Pgps were reconstituted into proteoliposomes for characterization of nucleotide (8-azido[α-^{32}P]ATP or TNP-ATP) binding and ATP hydrolysis.

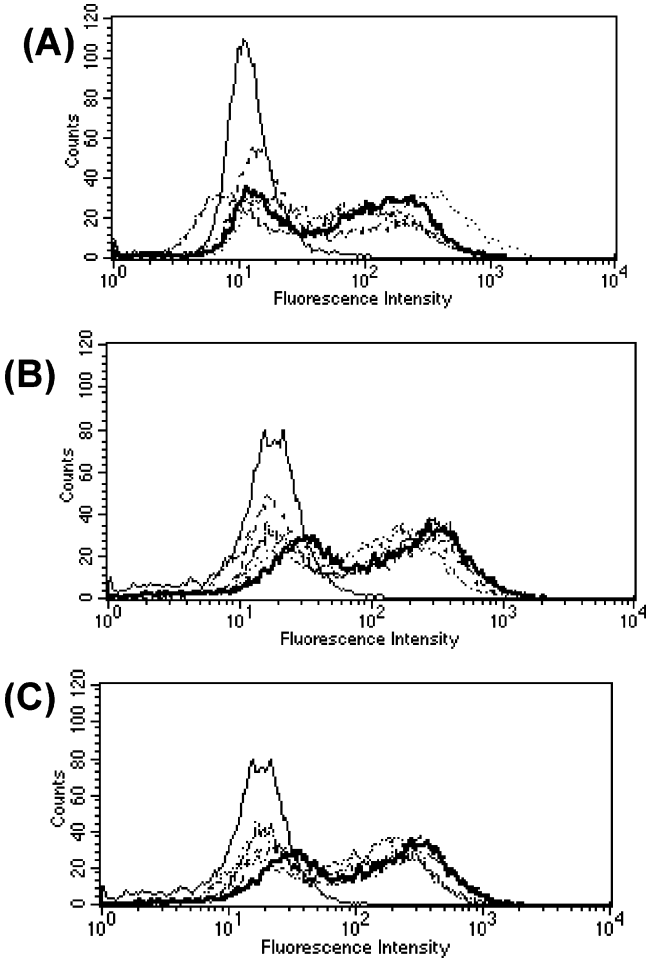

FIGURE 1: Expression of wild-type and mutant Pgps expressed in *Vaccinia* virus-infected HeLa cells. The cell surface expression of wild-type and mutant Pgps was assessed by staining Pgp in intact cells with human Pgp-specific monoclonal antibody MRK-16 (*33*) followed by flow cytometry as described in Experimental Procedures: (A) (thin line) pTM1, (thick line) wild type, (···) Y401A, (- - -) Y401C, (-·-) Y401W, and (-···) Y401F, (B) (thin line) pTM1, (thick line) wild type, (···) Y1044A, (- - -) Y1044C, (-·-) Y1044W, and (-···) Y1044F, and (C) (thin line) pTM1, (thick line) wild type, (···) Y401A/Y1044A, (- - -) Y401C/Y1044C, (-·-) Y401W/Y1044W, and (-···) Y401F/Y1044F.

Cell Surface Expression and Transport Function of Wild-Type and Tyrosine Mutant Pgps. The mutant Pgps with substitutions at Y401 and/or Y1044 were characterized in a *Vaccinia* virus-based expression system. HeLa cells infected and/or transfected with the wild-type and all mutant Pgps showed comparable cell surface expression as assessed by staining with human Pgp-specific monoclonal antibody MRK16 that recognizes an external epitope in a flow cytometry assay (Figure 1 and Table 1). Similarly, immunoblotting with Pgp-specific monoclonal antibody C219 showed similar levels of Pgp in crude membranes of HeLa cells expressing the wild-type and mutant proteins (data not shown). The functional status of the wild-type and mutant Pgps was assessed using a calcein-AM efflux assay. Figure 2 illustrates that in a flow cytometry assay HeLa cells expressing wild-type Pgp show a reduced level of accumulation of fluorescent calcein, whereas cells expressing equivalent amounts of Y401L and Y401C mutant Pgps show partial (30−50%) transport function (Table 1). The transport function is abrogated in Y401A mutant Pgp (Figure 2A), but Y401F and Y401W show the same transport activity as wild-type Pgp (Figure 2B,C). The results show that Y401 plays an important role in Pgp transport function and other aromatic amino acid residues can substitute for this tyrosine residue. We also studied the effect of substitution of Y1044 with A, C, F, and W in the C-terminal NBD. Transport of calcein-AM is abolished in mutants Y1044A and Y1044C (Figure 2A and Table 1), whereas the Y1044F and Y1044W mutants exhibited transport activity comparable to that of wild-type Pgp (Figure 2B,C). These results demonstrate that the tyrosine residue 25 amino acids upstream of the Walker A motif in both NBDs plays an important role in Pgp transport function. Furthermore, it would be expected that the substitution of both Y401 and Y1044 with A and C (Y401A/Y1044A and Y401C/Y1044C) would abrogate function, whereas substitutions with F and W in both NBDs (Y401F/Y1044F and Y401W/Y1044W) would retain functionality. However, we found that Y401W/Y1044W double mutant Pgp exhibited a complete loss of function, measured as efflux of calcein-AM. We also found loss of function in mutants Y401A/Y1044W and Y401C/Y1044W. However, mutants Y401F/

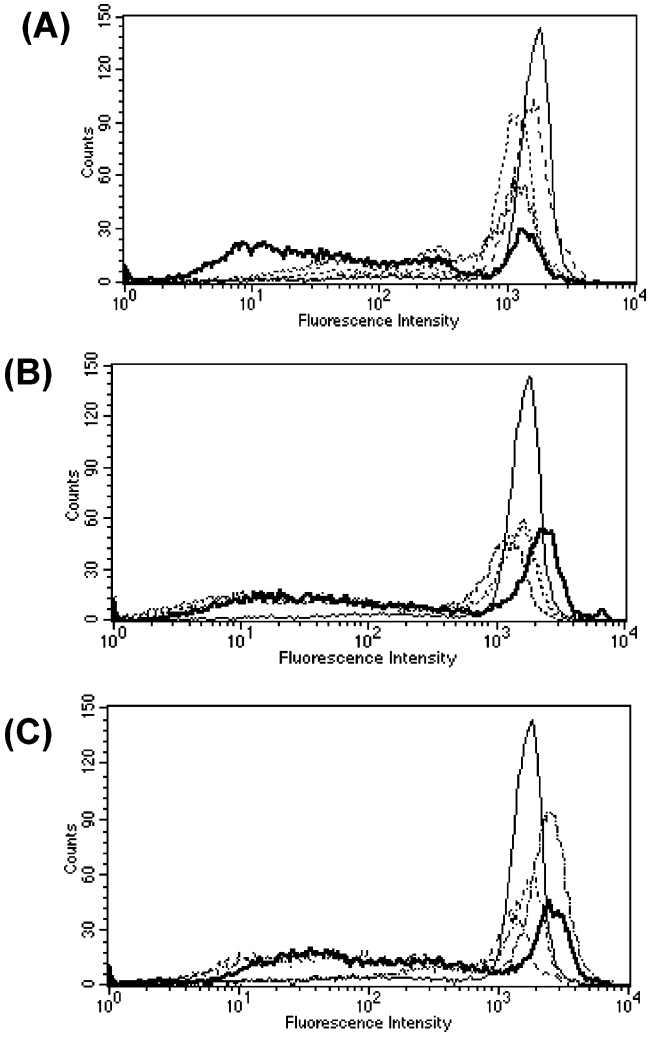

FIGURE 2: Transport function of wild-type and mutant Pgps using fluorescent substrate calcein-AM. Calcein-AM efflux mediated by wild-type and mutant Pgps was monitored by flow cytometry as described in Experimental Procedures: (A) (thin line) pTM1, (thick line) wild type, (···) Y401A, (- - -) Y1044A, and (-···) Y401A/Y1044A, (B) (thin line) pTM1, (thick line) wild type, (···) Y401F, (- - -) Y1044F, and (-···) Y401F/Y1044F, and (C) (thin line) pTM1, (thick line) wild type, (···) Y401W, (- - -) Y1044W, and (-···) Y401W/Y1044W.

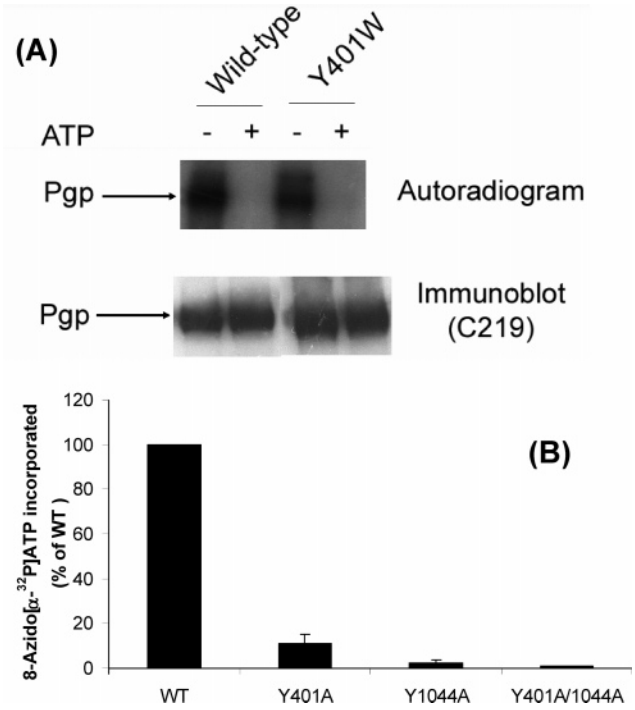

FIGURE 3: Binding of 8-azido[α-^{32}P]ATP to wild-type and mutant Pgps. (A) Crude membranes prepared from HighFive insect cells overexpressing the wild type or the Y401W mutant Pgp were incubated with 10 μM (with 5−10 μCi/nmol) 8-azido[α-^{32}P]ATP in the absence (−) or presence (+) of 10 mM ATP in the ATPase assay buffer as described in Experimental Procedures, photo-cross-linked, and separated on a 7% gel. The same samples were probed with Pgp-specific monoclonal antibody C219, and the immunoblot of the same blot shown in the autoradiogram is given below the autoradiogram. Experimental conditions are given on each autoradiogram. (B) Binding of 8-azido[α-^{32}P]ATP to purified and reconstituted wild-type and mutant Pgps (1−7 μg of protein/assay) was monitored as described for panel A. The 8-azido[α-^{32}P]ATP incorporated into wild-type and mutant Pgps in proteoliposomes was quantified using a phosphorimager, as described in Experimental Procedures. The mean values ± the standard deviation from three independent experiments are shown.

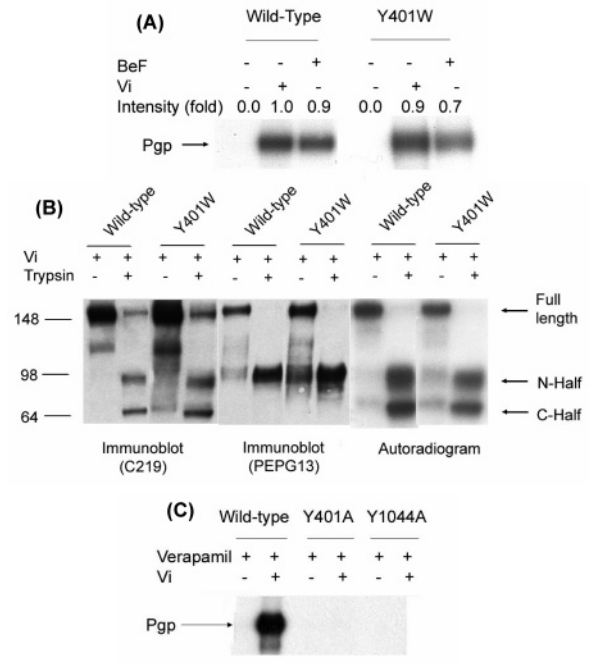

FIGURE 4: Trapping of 8-azido[α-^{32}P]ADP in wild-type and mutant Pgps and distribution of trapped nucleotides in the N-terminal and C-terminal ATP sites. (A) Vi- or BeF_x-induced trapping of 8-azido-[α-^{32}P]ADP in wild-type or Y401W mutant Pgp was monitored as described in Experimental Procedures. The autoradiogram depicts 8-azido[α-^{32}P]ADP incorporated into the wild-type and Y401W mutant protein in the presence and absence of Vi or BeF_x. (B) Distribution of trapped 8-azido[α-^{32}P]ADP in the N- and C-ATP sites of wild-type and Y401W mutant Pgp. Vi-induced trapping was carried out as described above, and samples were subjected to mild trypsinization, as described previously (*34*). Following electrophoresis and transfer to a nitrocellulose membrane, the samples were probed with Pgp polyclonal antisera PEPG-13 (*36*) or Pgp-specific monoclonal antibody C219, and the same blots were exposed to X-ray film to obtain the signal associated with 8-azido-[α-^{32}P]ADP. Experimental conditions are given in each panel. (C) Vi-induced nucleotide trapping was not observed with Y401A or Y1044A mutant Pgp. Wild-type and Y401A and Y1044A mutant Pgps were purified and reconstituted into proteoliposomes as described in Experimental Procedures. Proteoliposomes containing wild-type (20 μg of protein/mL) or Y401 and Y1044A mutant Pgps (150 μg of protein/mL) were incubated at 37 °C with 50 μM 8-azido[α-^{32}P]ATP in the presence of 50 μM verapamil and in the presence and absence of 0.3 mM Vi for 10 min. The samples were then processed as described in Experimental Procedures. An autoradiogram from a typical experiment is shown. Similar results were obtained in two more experiments.

Y1044W and Y401W/Y1044F were functional (Table 1). The substitution of tyrosine with tryptophan is tolerated at either the N- or C-terminal ATP sites but not in both NBDs, most likely due to the bulkiness of the tryptophan residue. Moreover, an asymmetric substitution where one of the tyrosine residues is replaced with a tryptophan and the other with phenylalanine is also well-tolerated.

Binding of 8-Azido[α-^{32}P]ATP to Wild-Type, Y401A, Y1044A, Y401A/Y1044A, Y401W, Y401C, and Y401L Mutant Pgps. To examine the role of the tyrosine residue in the nucleotide binding properties of Pgp, we used crude membranes prepared from HighFive insect cells infected with baculovirus containing the wild-type and mutant Pgps. We monitored binding of 8-azido[α-^{32}P]ATP to wild-type and mutant Pgps (Figure 3). Quantification of the radiolabel signal shows that the amount of 8-azido[α-^{32}P]ATP incorporated in Y401W is approximately 80% of that in wild-type Pgp. However, incorporation of 8-azido[α-^{32}P]ATP was drastically attenuated in the Y401A, Y1044A, and Y401A/1044A mutant Pgps, compared to that in wild-type Pgp (Figure 3B). The level of 8-azido[α-^{32}P]ATP incorporated into Y401A, Y1044A, and Y401A/Y1044A equaled 10−15, 3−5, and ∼1% (undetectable level), respectively. In Y401L and Y401C mutants, 30−50% of the azidonucleotide was incorporated.

Trapping of 8-Azido[α-^{32}P]ADP into Wild-Type, Y401A, Y1044A, Y401A/Y1044A, and Y401W Mutant Pgps. The BeF_x- or Vi-induced, pre- or posthydrolysis transition state Pgp·Mg-8-azido[α-^{32}P]ADP·BeF_x or Pgp·Mg-8-azido[α-^{32}P]-ADP·Vi has been extensively used to understand the catalytic cycle of Pgp (*38*, *41*, *47*). It is important to determine if the substitutions of Y401 and Y1044 that permit nucleotide binding also allow the generation of this transition state, which is the next step in the catalytic cycle of Pgp-mediated ATP hydrolysis. In Figure 4A, we show that wild-type and Y401W Pgps trap equivalent levels of 8-azido[α-^{32}P]ADP, whereas in Y401A and Y1044A mutant Pgps, Vi-induced 8-azidoADP trapping was not detected even in the presence of 30 μM verapamil (Figure 4C). Consistent with photo-

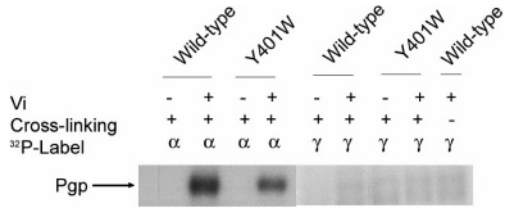

FIGURE 5: Vi-induced trapping of nucleotide in wild-type and Y401W mutant Pgps by incubating with 8-azido[α-^{32}P]ATP or 8-azido[γ-^{32}P]ATP. Vi-induced trapping was carried out with wild-type or mutant Y401W Pgp (0.5 mg of protein/mL) in ATPase assay buffer (see Experimental Procedures) using either 8-azido-[α-^{32}P]ATP (50 μM with 5 μCi/nmol) or 8-azido[γ-^{32}P]ATP (50 μM with 5 μCi/nmol) as the nucleotide. When 8-azido[γ-^{32}P]ATP was used, one of the samples was not photo-cross-linked as a control for kinase-mediated phosphorylation of Pgp (last lane). Samples were processed as described in the legend of Figure 3A. Reaction conditions are given on the autoradiogram of a representative experiment.

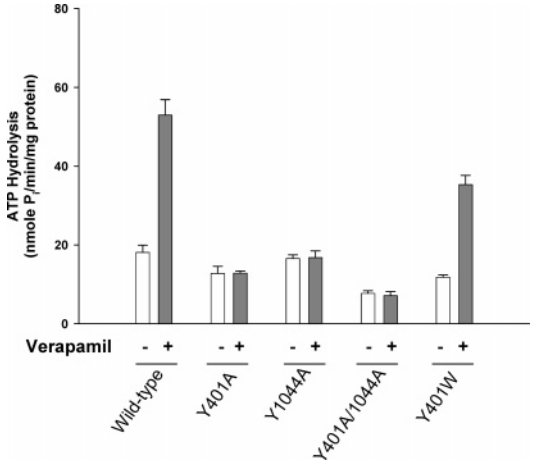

FIGURE 6: Basal and verapamil-stimulated ATPase activity of wild-type and mutant Pgps. Vi-sensitive ATP hydrolysis was assessed in crude membranes (100−200 μg of protein/mL) prepared from HighFive insect cells overexpressing wild-type and mutant Pgps by the colorimetric assay as described in Experimental Procedures. Assays were carried out in either the absence (white bars) or presence (gray bars) of 30 μM verapamil. Values are means, and the error bars represent standard deviations from three independent experiments. The control was crude membranes of HighFive cells infected with baculovirus lacking Pgp. Similar results were obtained when BeF_x instead of Vi was used as an inhibitor (data not shown).

cross-linking with 8-azidoATP at 4 °C, both Y401L and Y401C trap ~20% nucleotide in the presence of vanadate (Table 1). Similar results were obtained when BeF_x instead of Vi was used (data not shown). To determine whether the mutation in the N- or C-terminal NBD affects nucleotide trapping only at that site, the wild-type and Y401W Pgps were subjected to mild trypsin digestion following photo-cross-linking of trapped 8-azido[α-^{32}P]ADP in the presence of Vi as described in Experimental Procedures. Figure 4B shows the detection of immunoblot signals and incorporation of 8-azido[α-^{32}P]ADP in the same blot. An immunoblot of wild-type and Y401W Pgps after mild trypsinization was performed with polyclonal antibody PEPG-13 to detect the N-half of Pgp and Pgp-specific monoclonal antibody C219, which recognizes both halves of Pgp (*34*). Mild trypsinization of wild-type and Y401W Pgps showed that both the N- and C-terminal halves trap the radionucleotide (Figure 4B) to similar levels, indicating that the Y401W mutation does not affect the random selection of NBDs in initiating the catalytic cycle (*42*). These results also demonstrate that the substitution of Y401 with W does not affect photo-cross-linking with the 8-azido group of ATP.

To determine whether the trapped nucleotide is 8-azidoATP or 8-azidoADP, we incubated the wild-type and Y401W mutant Pgps in the presence of Vi with either 8-azido[α-^{32}P]ATP or 8-azido[γ-^{32}P]ATP (Figure 5). Following hydrolysis, the γ-^{32}P is cleaved, so there is no radioactive signal following photo-cross-linking in the Pgp band. We found that in both the wild type and the Y401W mutant there was no ^{32}P signal associated with the Pgp band when 8-azido[γ-^{32}P]ATP was used, suggesting that the trapped moiety is the nucleotide diphosphate, and this is indeed the posthydrolysis transition state.

To examine whether the differences in transport function were due to an alteration in the binding properties of transport substrate resulting from the Y401A, Y1044A, Y401A/Y1044A, and Y401W substitutions, we compared the photo-cross-linking of mutant Pgps with IAAP. [^{125}I]IAAP is the radiolabeled, photoactive analogue of Pgp drug substrate prazosin, which is also transported by Pgp (*48*) and has been extensively used to probe the drug binding sites of Pgp (*49*). Mutants Y401W, Y401A, Y1044A, and Y401A/Y1044A were all labeled with [^{125}I]IAAP at levels comparable to that of wild-type Pgp, and cyclosporine A inhibited IAAP incorporation in both wild-type and mutant Pgps (data not shown). These data suggest that mutation of the conserved tyrosine residue at positions 401 and 1044 does not affect photolabeling with transport substrate.

ATPase Activities of Wild-Type, Y401A, Y1044A, Y401A/Y1044A, and Y401W Pgps. The Vi-sensitive ATPase activity of wild-type and mutant Pgps was determined by assessing the liberation of inorganic phosphate using a colorimetric assay (*37*). The membranes prepared from control HighFive insect cells not expressing Pgp exhibit a Vi-sensitive basal activity of <5 nmol of P_i min^{-1} (mg of protein)$^{-1}$ and exhibit no verapamil-stimulated ATPase activity (data not shown). As shown in Figure 6, the wild-type Pgp as well as the Y401W mutant exhibited Vi-sensitive ATPase activity that was stimulated by verapamil. However, ATPase activity of the Y401A, Y1044A, and Y401A/Y1044A mutants was comparable to that of control HighFive cells not expressing Pgp. Moreover, verapamil had no effect on this activity. Other drug substrates such as vinblastine and valinomycin also gave comparable results, stimulating ATP hydrolysis only in the wild-type Pgp and the Y401W mutant (data not given). Similar results were also obtained when Vi was replaced with BeF_x for inhibition of Pgp-mediated ATP hydrolysis (data not shown). Although it is clear that mutant Y401W can hydrolyze ATP, the level of activity when 5 mM ATP is used is in the range of 60−75%, compared to that of wild-type protein. It was important to determine whether the kinetics of the ATP hydrolysis or affinity for nucleotide had been altered in any way. Thus, we determined the K_m(ATP) for wild-type and mutant Y401W Pgps both in the presence and in the absence of 30 μM verapamil. ATPase activities in the absence and presence of verapamil as a function of ATP concentration are shown in Figure S1 of the Supporting Information (panels A and B, respectively). The kinetic parameters of ATP hydrolysis by wild-type and Y401W mutant Pgp derived from the data in Figure S1 of the Supporting Information indicate that the maximal velocity

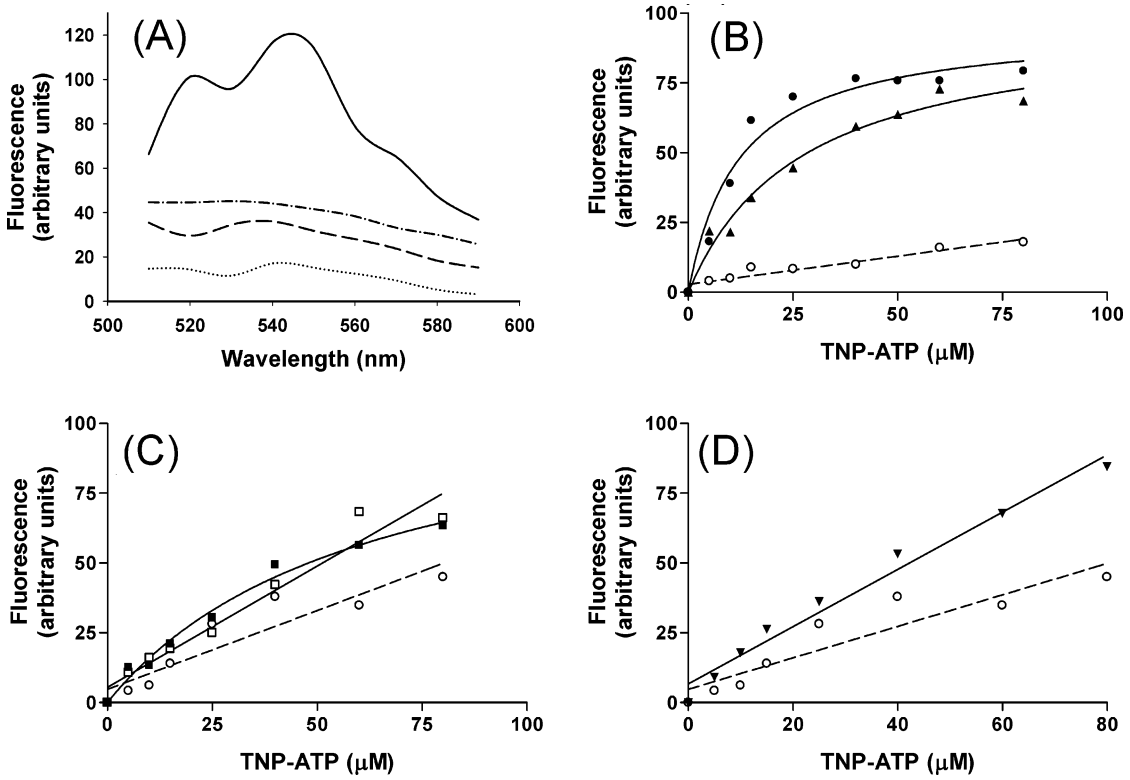

FIGURE 7: Binding of TNP-ATP to proteoliposomes containing purified wild-type, Y401W, Y401A, Y1044A, and Y401A/Y1044A mutant Pgps. (A) Emission scans (excitation at 408 nm and emission at 500−600 nm) of TNP-ATP (50 μM) in buffer alone or in the presence of liposomes or proteoliposomes containing wild-type Pgp were obtained. Scans represent TNP-ATP alone in assay buffer (•••) and in the presence of an equal volume of liposomes (- - -) and proteoliposomes containing purified wild-type Pgp (25 μg of protein/mL) in the absence (—) and presence (-•-_) of 10 mM ATP as described previously (*66*). (B−D) The affinity of TNP-ATP for wild-type (●) and Y401W mutant Pgp (▲) (20−25 μg of protein/mL), Y401A (■) and Y1044A (□) mutant Pgps (50−100 μg of protein/mL), double mutant Y401A/Y1044A Pgp (100 μg of protein/mL) (▼), and liposomes (○) (dashed line in panels B−D) was determined by using increasing concentrations of TNP-ATP. Fluorescence (excitation at 408 nm and emission at 560 nm) was measured as described in Experimental Procedures in the presence of increasing concentrations of TNP (2.5−80 μM), and each data point is the difference between the fluorescence in the absence and presence of excess ATP. In panels B−D, the lines represent the best fit for the data either by linear or nonlinear least-squares regression analysis using GraphPad Prism version 2.0. The results from a typical experiment are shown, and similar results were obtained in three additional experiments.

of ATP hydrolysis by both the Y401W mutant and the wild-type protein is in the same range. However, the K_m(ATP) for wild-type Pgp is 1.16 mM, versus 2.44 mM for the mutant Pgp in the absence of verapamil ($p < 0.05$). Similarly, in the presence of verapamil, the K_m(ATP) values for wild-type and mutant Pgps are 0.80 and 2.62 mM, respectively ($p < 0.005$). These results suggest that though there is a small decrease in the affinity for ATP in the Y401W mutant, this substitution is tolerated by Pgp and unlikely to have any effect under physiological conditions. This conclusion is strengthened by the findings that the V_{max} values for wild-type and mutant Y401W Pgps are comparable. This is also consistent with the similar transport activities in both wild-type and Y401W mutant Pgps (Figure 2 and Table 1).

Binding of TNP-ATP to Wild-Type, Y401A, Y1044A, Y401A/Y1044A, and Y401W Pgps. TNP-ATP, a fluorescent analogue of ATP, has been used to characterize the relative affinities of ATP sites (*42*, *50*). An increase in fluorescence intensity and a small blue shift in the emission (from 550 to 530 nm) accompany the binding of TNP-ATP to the ATP or NBD sites. We monitored the fluorescence emission spectrum of TNP-ATP in the presence or absence of proteoliposomes reconstituted with purified Pgp using liposomes as a negative control. The differential spectra correspond to the fluorescence of bound TNP-ATP and exhibited a maximum emission at 540 nm (Figure 7A). Scans taken in the presence of Pgp showed that the magnitude of the fluorescence signal was significantly decreased in the presence of excess (10 mM) ATP. Therefore, we measured the fluorescence using increasing concentrations of TNP-ATP in the presence of Pgp-containing proteoliposomes in the absence and presence of excess ATP, and the fluorescence measurements taken in the presence of Pgp were corrected for nonspecific binding by subtracting the fluorescence signal acquired in the presence of excess ATP. The increase in fluorescence upon binding of TNP-ATP to wild-type and Y401W mutant Pgps was concentration-dependent and saturable (Figure 7B), and the apparent K_d(TNP-ATP) for the mutant Pgp, Y401W, was 32.8 μM compared to a value of 11.2 μM for wild-type Pgp. Thus, though mutant Y401W hydrolyzes ATP and retains transport function, the affinity for ATP is reduced 2−2.5-fold. However, the concentration required for half-maximal binding of TNP-ATP to Y401A mutant Pgp was considerably higher than that for the wild type (105.5 μM, Figure 7C). Furthermore, the binding of TNP-ATP to Y1044A and Y401A/Y1044A mutant Pgs was not saturable up to 100 μM (Figure 7C,D), and for this reason, we could not determine the affinity of the fluorescent nucleotide for these mutants. It is worth noting that for experiments in panels C and D of Figure 7, 2−4 times more protein, Y401A, Y1044A, and Y401A/Y1004A mutant Pgps, was used to obtain signal above the liposomal

level. It is clear that even in the case of the Y401A mutant, the apparent K_d value is significantly underestimated. Photocross-linking with 8-azido[α-^{32}P]ATP (Figure 3B) and TNP-ATP binding assays show that the substitution of either Y401 or Y1044 with alanine significantly affects the binding of nucleotide to Pgp, suggesting that there might be cooperativity between both NBDs even for binding of nucleotides. Similar results were also obtained with Y401L and Y401C mutants (see Table 1). The partial activity is observed only with Y401C in NBD1 and not with Y1044C in NBD2, suggesting that there might be cooperativity and slight asymmetry in NBD1 and NBD2. The aromatic residue is always Y at this position in NBD2 of ABC transporters (see Table 1 in ref *46*), consistent with our findings that a nonaromatic residue at this position in NBD2 is not even partially tolerated. Further work on these and other substitutions of the tyrosine residue at positions 401 and 1044 will be required to address this issue.

[α-^{32}P]ATP Hydrolysis by Wild-Type, Y401A, Y1044A, and Y401A/Y1044A Mutant Pgps. The ATPase activity of the purified wild-type and mutant Pgps reconstituted into proteoliposomes was measured with a very sensitive assay using [α-^{32}P]ATP and the separation of [α-^{32}P]ATP and [α-^{32}P]-ADP via TLC as described in Experimental Procedures. The specific activity of wild-type Pgp was 530 nmol of ADP min^{-1} (mg of protein)$^{-1}$ and increased to 1030 nmol of[α-^{32}P]ADP min^{-1} (mg of protein)$^{-1}$ in the presence of 50 μM verapamil (Table S2 of the Supporting Information), which is comparable to levels obtained in earlier studies (*37*−*39*). The separation of [α-^{32}P]ATP and [α-^{32}P]ADP following hydrolysis reaction by wild-type and mutant Pgp on a TLC is depicted in Figure S2 of the Supporting Information. Consistent with the results with crude membrane preparations, we found that ATP hydrolysis was completely abolished by substitution of tyrosine with alanine at position 401 and/or 1044 in proteoliposomes reconstituted with purified mutant proteins. In these experiments, we used a 10-fold higher concentration of mutant Pgps (100−200 μg/mL) than of wild-type protein (10−20 μg/mL) to be able to detect even very low levels of nucleotide hydrolysis.

DISCUSSION

The NBD of an ABC transport protein is composed of the Walker A and B motifs, the signature motif (also termed the LSGGQ motif, linker peptide, or C motif), and the D-, H-, and Q-loops. On the basis of recent studies, the general architecture of an ATP site appears to be a "nucleotide-sandwich dimer" (*28*, *51*, *52*). In such a dimer, the ATP is bound along the interface, flanked by the Walker A and B motifs of one subunit and the signature motif and D-loop of the other (*14*, *28*). Previous studies involving site-directed mutagenesis (*3*, *14*, *34*, *53*−*59*) and the recent work on resolution of structures of NBDs with bound nucleotide (Table S3 of the Supporting Information) help elucidate specific roles for several highly conserved amino acid residues within the ABC. Several groups have studied the role of these residues, which appear to be critical for ATP hydrolysis as well as for communication with drug−substrate sites (*60*−*63*). There has not, however, been a systematic approach to determining if there is a common region in ABC transporters that facilitates such interactions. Data mining with RPS-BLAST identified 18 514 ABC domains in a set of all nonredundant proteins. The sequence alignment of these domains indicated that 88.1% (or 16 312) of NBDs possess an aromatic amino acid 25 (±2) residues upstream of the Walker A motif (Table S1 of the Supporting Information). We therefore undertook a comprehensive analysis of the conserved aromatic residues (at positions 401 and 1044) in both NBDs of Pgp. We mutated the conserved Y residue in both NBDs either singly or together. The tyrosine residue was replaced with W, F, C, or A. The C residue was chosen because an equivalent mutation has been demonstrated to be functional in MRP1 and CFTR (*24*, *25*). In this study, we found that substitution of Y401 and Y1044 with C and A does not affect the expression of protein but impairs the transport function of Pgp in a *Vaccinia* virus expression system, suggesting that these residues have an important role in ATP binding and ATP hydrolysis. Substitution of the Y residue with F or W has no significant effect on transport function, indicating that any aromatic residue at these positions in Pgp can be tolerated. Although the individual substitution of the conserved tyrosine residues with tryptophan in the two NBDs does not affect function, simultaneous substitution of both tyrosine residues results in the loss of function (these results are summarized in Table 1). This is probably because of the steric hindrance of tryptophan residues, which have large indole side chains and are the bulkiest of all amino acids.

To study ATP binding and hydrolysis in detail, we used the baculovirus-infected HighFive insect cell system. The purified wild-type and mutant proteins were reconstituted into liposomes prepared with a lipid mixture containing phospholipids and cholesterol mimicking the mammalian plasma membrane lipid composition (*39*) by removing detergent with dialysis. Y401W mutant Pgp in the reconstituted system exhibits properties similar to those of the wild-type protein except for a somewhat reduced affinity for ATP. On the other hand, the Y → A mutants do not show transport or ATP hydrolysis and the Y401A mutant exhibited significantly attenuated (<20%) 8-azido[α-^{32}P]ATP and negligible TNP-ATP binding (Table 1 and Figures 3B and 7C). However, Y1044A mutant Pgp does not exhibit nucleotide (TNP-ATP and 8-azido[α-^{32}P]ATP) binding (Figures 3B and 7C). These findings suggest that the NBDs in Pgp exhibit cooperativity for nucleotide binding as well as for hydrolysis. It is important to note that the aromatic residue in NBD2 is universally a tyrosine, whereas there is some diversity in NBD1. Consistent with this view is the fact that while mutants Y401L and Y401C are partially (30−50%) functional, mutants Y1044C and Y401C/Y1044C are completely nonfunctional (Table 1). These findings suggest that the ABC domains of ABC transporters exhibit some structural differences. Previous work with bacterial HisP demonstrated that substitution of Y16 with S resulted in a loss of transport function (*23*). The biochemical studies described here thus demonstrate an important role for the conserved tyrosine residues of Pgp in nucleotide binding and not just for cross-linking with 8-azido[α-^{32}P]ATP, as suggested previously (*26*). To further understand the interactions between the nucleotide and protein, the NBD1−NBD2 dimer of Pgp was modeled on the ATP-bound structure of the E171Q mutant NBD of MJ0796 (*28*) using O (*64*). The model in Figure 8 shows that ATP is present at the interphase of the nucleotide-sandwich dimer formed by the Walker A and B motifs of

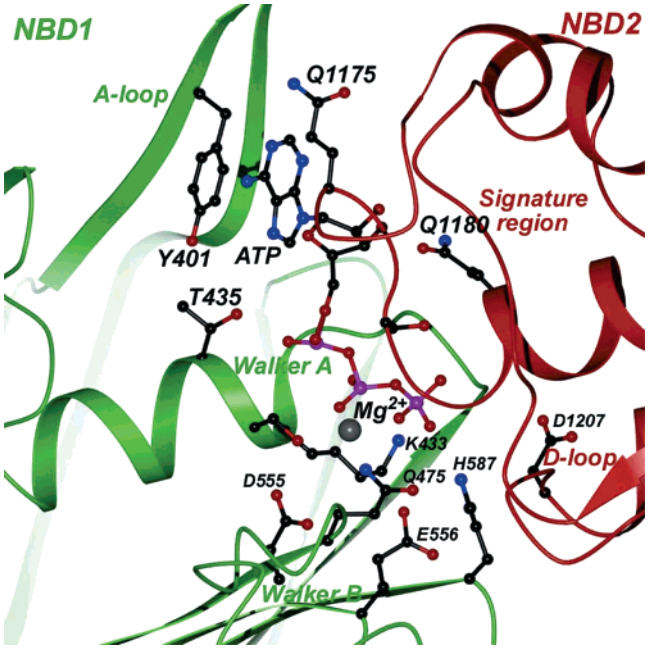

FIGURE 8: Atomic model of the NBD1−NBD2 dimer of Pgp showing the stacking of Tyr401 with the adenine base of ATP. This atomic model of the NBD1−NBD2 dimer was generated on the basis of the coordinates from the crystal structure of the MJ0796 E171Q mutant NBD (PDB entry 1L2T) (*28*) using O (*64*) by mapping the NBD1 and NBD2 sequences to either subunit. The resulting dimeric ABC was subjected to a few cycles of molecular dynamics in CNS, and the final model was checked with PROCHECK. The secondary structure elements of the N-terminal NBD (NBD1) are depicted as the ribbon diagrams in green, and those from the C-terminal NBD (NBD2) are colored red. Important sequence motifs such as the Walker A motif, the Walker B motif, the H-loop, the signature region, and the D-loop are labeled accordingly. The bound ATP moiety and some of the interacting residues are shown as the ball-and-stick model and are labeled, where carbon atoms are colored black, oxygen atoms red, nitrogen atoms blue, and phosphate atoms magenta. The Mg^{2+} ion is shown as a metallic sphere. Y401 in the A-loop stacks against the adenine ring of ATP. For clarity, only one composite ATP site is shown. This figure was prepared using GLR (www.convent.nci.nih.gov/glr).

NBD1 and the signature region and the D-loop of NBD2. The signature region of NBD2 of Pgp has been shown to be in the proximity of the Walker A motif in NBD1 (*59*). The homology model of the NBD1−NBD2 dimer depicted in Figure 8 clearly shows that Y401 stacks with the adenine ring of ATP, most likely through $\pi-\pi$ interactions (*21*). Similar stacking of Y401 with the adenine ring of ATP was also seen when the NBD1−NBD2 dimer of Pgp was modeled on the ATP-bound structure of the H662A mutant of HlyB (ref *65* and data not shown). Homology modeling of NBD1 of Pgp based on the dimer of the MJ0796 E171Q mutant suggests that replacement of Y with L is tolerated to some extent due to hydrophobic interaction between the leucine residue and the adenine base. The distance between Cδ1 of leucine and C6 of the adenine base is 2.75 Å, and the distance between Cδ1 of leucine and C5 of the adenine base is 2.66 Å. On the other hand, in the Y401C mutant, the S group of the C residue interacts with C6 of the adenine base through hydrogen bonding (distance of 3.3 Å). These analyses suggest that both hydrophobic or hydrogen bond interactions of the residue at this position are not sufficient to support ATP binding and hydrolysis to the same extent as the aromatic acid in the wild-type protein. It will be worthwhile to test whether substitution of Y401 with R will result in cation$-\pi$ interaction with the adenine base.

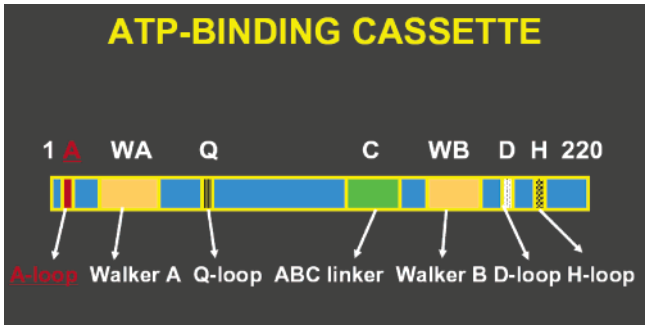

FIGURE 9: Schematic of the ABC showing conserved motifs, including the subdomain, the A-loop. A typical ABC or NBD domain is comprised of ~220 residues, and subdomains Walker A (WA) and Walker B (WB), the ABC linker (C region), and D-, H-, and Q-loops are depicted. The aromatic residue at a position ~25 amino acids upstream of the Walker A motif, which interacts with the adenine base of ATP, appears to mark the boundary at the amino terminus of the ABC domain. Due to its highly conserved nature and importance in ATP binding, this residue should be considered as an integral part of the ABC domain. To emphasize its importance, we named this residue the A-loop (aromatic residue interacting with the adenine base), depicted as A and A-loop.

Large-scale data mining, sequence alignments (Table S1 of the Supporting Information), and generation of the Sequence Logo (*46*) all suggest a highly conserved aromatic residue 25 (±2) amino acids upstream of the Walker A motif. In addition, all 11 structures of ABC domains except for Rad50 and MutS clearly show interaction between the adenosine ring of the nucleotide and the conserved aromatic residue (Table S3 of the Supporting Information and references therein). Previous studies have demonstrated the role of an aromatic residue in individual ABC transporters (Table S3 of the Supporting Information), and one study has reported a structural domain termed the "Y-loop" with a conserved Y residue (*20*). However, not all ABC domains have a conserved Y residue (see Table S1 of the Supporting Information; only 55% ABCs have a Y residue). In addition, none of the previous studies systematically substituted the given aromatic residue with two other aromatic residues or with alanine in both NBDs individually and together to conclusively demonstrate the importance of this aromatic residue for ATP binding. Here, we substituted Y residues in both NBDs (Y401 and Y1044) of Pgp with W, F, A, C, or L (at position 401 only) to clearly identify the need for an aromatic residue at this position for proper ATP binding and hydrolysis. In addition to the extensive biochemical characterization of these mutations in Pgp, we employed large-scale data mining, sequence alignment, analysis of structures of nucleotide-bound NBDs, and homology modeling to demonstrate the critical role of this conserved subdomain in the ABC cassette. To emphasize its importance in binding the adenine ring of ATP, we named this subdomain the A-loop (aromatic residue involved in interaction with an adenine base). Thus, this A-loop should be considered as an integral part of the NBD in ABC transporters. A revised schematic of the ABC domain that incorporates this subdomain (A-loop) is depicted in Figure 9.

An analysis of nucleotide protein interactions in 68 nonredundant, high-resolution crystal structures of nucle-

otide-binding proteins, including ATPases, kinases, and ABC proteins, by Mao and co-workers (*21*) suggests that in addition to $\pi-\pi$ interactions between aromatic residues and nucleotides, hydrogen bonding is also involved. Thus, further work in identifying residues (most likely downstream of the Y residues, S/T and R as YPS/TR in the A-loop are highly conserved in mammalian and avian Pgps) involved in hydrogen bonding with the adenine base in NBDs will provide a more comprehensive understanding of the forces involved in binding of the nucleotide to Pgp and other ABC transport proteins.

ACKNOWLEDGMENT

We thank Dr. Michael M. Gottesman, members of MDR group, and Drs. Peter Jones and Anthony George (University of Technology, Sydney, Australia) for helpful discussions. We also thank George Leiman for editorial assistance in the preparation of the manuscript.

SUPPORTING INFORMATION AVAILABLE

Additional tables (S1−S3) and figures (S1 and S2) showing results of data mining, ATP hydrolysis activity of wild-type and mutant Pgps and a list of structures of nucleotide-bound NBDs, in which an aromatic residue interacts with the adenine base of nucleotide as described in the text. This material is available free of charge via the Internet at http://pubs.acs.org.

REFERENCES

1. Gottesman, M. M., Fojo, T., and Bates, S. E. (2002) Multidrug resistance in cancer: Role of ATP-dependent transporters, *Nat. Rev. Cancer 2*, 48−58.
2. Ambudkar, S. V., Kimchi-Sarfaty, C., Sauna, Z. E., and Gottesman, M. M. (2003) P-glycoprotein: From genomics to mechanism, *Oncogene 22*, 7468−85.
3. Ambudkar, S. V., Dey, S., Hrycyna, C. A., Ramachandra, M., Pastan, I., and Gottesman, M. M. (1999) Biochemical, cellular, and pharmacological aspects of the multidrug transporter, *Annu. Rev. Pharmacol. Toxicol. 39*, 361−98.
4. Chen, C. J., Chin, J. E., Ueda, K., Clark, D. P., Pastan, I., Gottesman, M. M., and Roninson, I. B. (1986) Internal duplication and homology with bacterial transport proteins in the mdr1 (P-glycoprotein) gene from multidrug-resistant human cells, *Cell 47*, 381−9.
5. Gottesman, M. M., Pastan, I., and Ambudkar, S. V. (1996) P-Glycoprotein and multidrug resistance, *Curr. Opin. Genet. Dev. 6*, 610−7.
6. Hrycyna, C. A., Airan, L. E., Germann, U. A., Ambudkar, S. V., Pastan, I., and Gottesman, M. M. (1998) Structural flexibility of the linker region of human P-glycoprotein permits ATP hydrolysis and drug transport, *Biochemistry 37*, 13660−73.
7. Hyde, S. C., Emsley, P., Hartshorn, M. J., Mimmack, M. M., Gileadi, U., Pearce, S. R., Gallagher, M. P., Gill, D. R., Hubbard, R. E., and Higgins, C. F. (1990) Structural model of ATP-binding proteins associated with cystic fibrosis, multidrug resistance and bacterial transport, *Nature 346*, 362−5.
8. Gottesman, M. M., and Ambudkar, S. V. (2001) Overview: ABC transporters and human disease, *J. Bioenerg. Biomembr. 33*, 453−8.
9. Horio, M., Gottesman, M. M., and Pastan, I. (1988) ATP-dependent transport of vinblastine in vesicles from human multidrug-resistant cells, *Proc. Natl. Acad. Sci. U.S.A. 85*, 3580−4.
10. Hung, L. W., Wang, I. X., Nikaido, K., Liu, P. Q., Ames, G. F., and Kim, S. H. (1998) Crystal structure of the ATP-binding subunit of an ABC transporter, *Nature 396*, 703−7.
11. Yuan, Y. R., Blecker, S., Martsinkevich, O., Millen, L., Thomas, P. J., and Hunt, J. F. (2001) The crystal structure of the MJ0796 ATP-binding cassette. Implications for the structural consequences of ATP hydrolysis in the active site of an ABC transporter, *J. Biol. Chem. 276*, 32313−21.
12. Yuan, Y. R., Martsinkevich, O., and Hunt, J. F. (2003) Structural characterization of an MJ1267 ATP-binding cassette crystal with a complex pattern of twinning caused by promiscuous fiber packing, *Acta Crystallogr. D59*, 225−38.
13. Bohm, A., Diez, J., Diederichs, K., Welte, W., and Boos, W. (2002) Structural model of MalK, the ABC subunit of the maltose transporter of *Escherichia coli*: Implications for mal gene regulation, inducer exclusion, and subunit assembly, *J. Biol. Chem. 277*, 3708−17.
14. Chen, J., Lu, G., Lin, J., Davidson, A. L., and Quiocho, F. A. (2003) A tweezers-like motion of the ATP-binding cassette dimer in an ABC transport cycle, *Mol. Cell 12*, 651−61.
15. Verdon, G., Albers, S. V., Dijkstra, B. W., Driessen, A. J., and Thunnissen, A. M. (2003) Crystal structures of the ATPase subunit of the glucose ABC transporter from *Sulfolobus solfataricus*: Nucleotide-free and nucleotide-bound conformations, *J. Mol. Biol. 330*, 343−58.
16. Reyes, C. L., and Chang, G. (2005) Structure of the ABC transporter MsbA in complex with ADP•vanadate and lipopolysaccharide, *Science 308*, 1028−31.
17. Lewis, H. A., Buchanan, S. G., Burley, S. K., Conners, K., Dickey, M., Dorwart, M., Fowler, R., Gao, X., Guggino, W. B., Hendrickson, W. A., Hunt, J. F., Kearins, M. C., Lorimer, D., Maloney, P. C., Post, K. W., Rajashankar, K. R., Rutter, M. E., Sauder, J. M., Shriver, S., Thibodeau, P. H., Thomas, P. J., Zhang, M., Zhao, X., and Emtage, S. (2004) Structure of nucleotide-binding domain 1 of the cystic fibrosis transmembrane conductance regulator, *EMBO J. 23*, 282−93.
18. Lewis, H. A., Zhao, X., Wang, C., Sauder, J. M., Rooney, I., Noland, B. W., Lorimer, D., Kearins, M. C., Conners, K., Condon, B., Maloney, P. C., Guggino, W. B., Hunt, J. F., and Emtage, S. (2005) Impact of the ΔF508 mutation in first nucleotide-binding domain of human cystic fibrosis transmembrane conductance regulator on domain folding and structure, *J. Biol. Chem. 280*, 1346−53.
19. Gaudet, R., and Wiley, D. C. (2001) Structure of the ABC ATPase domain of human TAP1, the transporter associated with antigen processing, *EMBO J. 20*, 4964−72.
20. Karcher, A., Buttner, K., Martens, B., Jansen, R. P., and Hopfner, K. P. (2005) X-ray structure of RLI, an essential twin cassette ABC ATPase involved in ribosome biogenesis and HIV capsid assembly, *Structure 13*, 649−59.
21. Mao, L., Wang, Y., Liu, Y., and Hu, X. (2004) Molecular determinants for ATP-binding in proteins: A data mining and quantum chemical analysis, *J. Mol. Biol. 336*, 787−807.
22. Polshakov, D., Rai, S., Wilson, R. M., Mack, E. T., Vogel, M., Krause, J. A., Burdzinski, G., and Platz, M. S. (2005) Photoaffinity labeling with 8-azidoadenosine and its derivatives: Chemistry of closed and opened adenosine diazaquinodimethanes, *Biochemistry 44*, 11241−53.
23. Shyamala, V., Baichwal, V., Beall, E., and Ames, G. F. (1991) Structure−function analysis of the histidine permease and comparison with cystic fibrosis mutations, *J. Biol. Chem. 266*, 18714−9.
24. Berger, A. L., and Welsh, M. J. (2000) Differences between cystic fibrosis transmembrane conductance regulator and HisP in the interaction with the adenine ring of ATP, *J. Biol. Chem. 275*, 29407−12.
25. Zhao, Q., and Chang, X. B. (2004) Mutation of the aromatic amino acid interacting with adenine moiety of ATP to a polar residue alters the properties of multidrug resistance protein 1, *J. Biol. Chem. 279*, 48505−12.
26. Sankaran, B., Bhagat, S., and Senior, A. E. (1997) Photoaffinity labelling of P-glycoprotein catalytic sites, *FEBS Lett. 417*, 119−22.
27. Senior, A. E. (1998) Catalytic mechanism of P-glycoprotein, *Acta Physiol. Scand. Suppl. 643*, 213−8.
28. Smith, P. C., Karpowich, N., Millen, L., Moody, J. E., Rosen, J., Thomas, P. J., and Hunt, J. F. (2002) ATP binding to the motor domain from an ABC transporter drives formation of a nucleotide sandwich dimer, *Mol. Cell 10*, 139−49.
29. Dean, M., and Annilo, T. (2005) Evolution of the ATP-Binding Cassette (ABC) Transporter Superfamily in Vertebrates, *Annu. Rev. Genomics Hum. Genet. 6*, 123−42.
30. Thompson, J. D., Higgins, D. G., and Gibson, T. J. (1994) CLUSTAL W: Improving the sensitivity of progressive multiple

sequence alignment through sequence weighting, position-specific gap penalties and weight matrix choice, *Nucleic Acids Res. 22*, 4673−80.
31. Ramachandra, M., Ambudkar, S. V., Gottesman, M. M., Pastan, I., and Hrycyna, C. A. (1996) Functional characterization of a glycine 185-to-valine substitution in human P-glycoprotein by using a *Vaccinia*-based transient expression system, *Mol. Biol. Cell 7*, 1485−98.
32. Gribar, J. J., Ramachandra, M., Hrycyna, C. A., Dey, S., and Ambudkar, S. V. (2000) Functional characterization of glycosylation-deficient human P-glycoprotein using a *Vaccinia* virus expression system, *J. Membr. Biol. 173*, 203−14.
33. Hamada, H., and Tsuruo, T. (1986) Functional role for the 170- to 180-kDa glycoprotein specific to drug-resistant tumor cells as revealed by monoclonal antibodies, *Proc. Natl. Acad. Sci. U.S.A. 83*, 7785−9.
34. Sauna, Z. E., Muller, M., Peng, X. H., and Ambudkar, S. V. (2002) Importance of the conserved Walker B glutamate residues, 556 and 1201, for the completion of the catalytic cycle of ATP hydrolysis by human P-glycoprotein (ABCB1), *Biochemistry 41*, 13989−4000.
35. Kartner, N., Evernden-Porelle, D., Bradley, G., and Ling, V. (1985) Detection of P-glycoprotein in multidrug-resistant cell lines by monoclonal antibodies, *Nature 316*, 820−3.
36. Bruggemann, E. P., Chaudhary, V., Gottesman, M. M., and Pastan, I. (1991) *Pseudomonas exotoxin* fusion proteins are potent immunogens for raising antibodies against P-glycoprotein, *BioTechniques 10*, 202−9.
37. Ramachandra, M., Ambudkar, S. V., Chen, D., Hrycyna, C. A., Dey, S., Gottesman, M. M., and Pastan, I. (1998) Human P-glycoprotein exhibits reduced affinity for substrates during a catalytic transition state, *Biochemistry 37*, 5010−9.
38. Kerr, K. M., Sauna, Z. E., and Ambudkar, S. V. (2001) Correlation between steady-state ATP hydrolysis and vanadate-induced ADP trapping in human P-glycoprotein. Evidence for ADP release as the rate-limiting step in the catalytic cycle and its modulation by substrates, *J. Biol. Chem. 276*, 8657−64.
39. Ambudkar, S. V., Lelong, I. H., Zhang, J., Cardarelli, C. O., Gottesman, M. M., and Pastan, I. (1992) Partial purification and reconstitution of the human multidrug-resistance pump: Characterization of the drug-stimulatable ATP hydrolysis, *Proc. Natl. Acad. Sci. U.S.A. 89*, 8472−6.
40. Schaffner, W., and Weissmann, C. (1973) A rapid, sensitive, and specific method for the determination of protein in dilute solution, *Anal. Biochem. 56*, 502−14.
41. Sauna, Z. E., Smith, M. M., Muller, M., and Ambudkar, S. V. (2001) Functionally similar vanadate-induced 8-azidoadenosine 5′-[α-^{32}P]diphosphate-trapped transition state intermediates of human P-glycoprotein are generated in the absence and presence of ATP hydrolysis, *J. Biol. Chem. 276*, 21199−208.
42. Sauna, Z. E., and Ambudkar, S. V. (2001) Characterization of the catalytic cycle of ATP hydrolysis by human P-glycoprotein. The two ATP hydrolysis events in a single catalytic cycle are kinetically similar but affect different functional outcomes, *J. Biol. Chem. 276*, 11653−61.
43. Dey, S., Ramachandra, M., Pastan, I., Gottesman, M. M., and Ambudkar, S. V. (1998) Photoaffinity labeling of human P-glycoprotein: Effect of modulator interaction and ATP hydrolysis on substrate binding, *Methods Enzymol. 292*, 318−28.
44. Ambudkar, S. V. (1998) Drug-stimulatable ATPase activity in crude membranes of human MDR1-transfected mammalian cells, *Methods Enzymol. 292*, 504−14.
45. Kozak, L., Gopal, G., Yoon, J. H., Sauna, Z. E., Ambudkar, S. V., Thakurta, A. G., and Dhar, R. (2002) Elf1p, a member of the ABC class of ATPases, functions as an mRNA export factor in *Schizosaccharomyces pombe*, *J. Biol. Chem. 277*, 33580−9.
46. Ambudkar, S. V., Kim, I. W., Xia, D., and Sauna, Z. E. (2006) The A-loop, a novel conserved aromatic acid subdomain upstream of the Walker A motif in ABC transporters, is critical for ATP binding, *FEBS Lett. 580*, 1049−55.
47. Urbatsch, I. L., Sankaran, B., Weber, J., and Senior, A. E. (1995) P-Glycoprotein is stably inhibited by vanadate-induced trapping of nucleotide at a single catalytic site, *J. Biol. Chem. 270*, 19383−90.
48. Maki, N., Hafkemeyer, P., and Dey, S. (2003) Allosteric modulation of human P-glycoprotein. Inhibition of transport by preventing substrate translocation and dissociation, *J. Biol. Chem. 278*, 18132−9.
49. Sauna, Z. E., Andrus, M. B., Turner, T. M., and Ambudkar, S. V. (2004) Biochemical basis of polyvalency as a strategy for enhancing the efficacy of P-glycoprotein (ABCB1) modulators: Stipiamide homodimers separated with defined-length spacers reverse drug efflux with greater efficacy, *Biochemistry 43*, 2262−71.
50. Liu, R., and Sharom, F. J. (1997) Fluorescence studies on the nucleotide binding domains of the P-glycoprotein multidrug transporter, *Biochemistry 36*, 2836−43.
51. Hopfner, K. P., Karcher, A., Shin, D. S., Craig, L., Arthur, L. M., Carney, J. P., and Tainer, J. A. (2000) Structural biology of Rad50 ATPase: ATP-driven conformational control in DNA double-strand break repair and the ABC-ATPase superfamily, *Cell 101*, 789−800.
52. Higgins, C. F., and Linton, K. J. (2004) The ATP switch model for ABC transporters, *Nat. Struct. Mol. Biol. 11*, 918−26.
53. Muller, M., Bakos, E., Welker, E., Varadi, A., Germann, U. A., Gottesman, M. M., Morse, B. S., Roninson, I. B., and Sarkadi, B. (1996) Altered drug-stimulated ATPase activity in mutants of the human multidrug resistance protein, *J. Biol. Chem. 271*, 1877−83.
54. Hrycyna, C. A., Ramachandra, M., Germann, U. A., Cheng, P. W., Pastan, I., and Gottesman, M. M. (1999) Both ATP sites of human P-glycoprotein are essential but not symmetric, *Biochemistry 38*, 13887−99.
55. Urbatsch, I. L., Gimi, K., Wilke-Mounts, S., and Senior, A. E. (2000) Investigation of the role of glutamine-471 and glutamine-1114 in the two catalytic sites of P-glycoprotein, *Biochemistry 39*, 11921−7.
56. Tombline, G., Bartholomew, L. A., Urbatsch, I. L., and Senior, A. E. (2004) Combined mutation of catalytic glutamate residues in the two nucleotide binding domains of P-glycoprotein generates a conformation that binds ATP and ADP tightly, *J. Biol. Chem. 279*, 31212−20.
57. Dean, M., Rzhetsky, A., and Allikmets, R. (2001) The human ATP-binding cassette (ABC) transporter superfamily, *Genome Res. 11*, 1156−66.
58. Jones, P. M., and George, A. M. (2004) The ABC transporter structure and mechanism: Perspectives on recent research, *Cell. Mol. Life Sci. 61*, 682−99.
59. Loo, T. W., Bartlett, M. C., and Clarke, D. M. (2002) The "LSGGQ" motif in each nucleotide-binding domain of human P-glycoprotein is adjacent to the opposing Walker A sequence, *J. Biol. Chem. 277*, 41303−6.
60. Hoof, T., Demmer, A., Hadam, M. R., Riordan, J. R., and Tummler, B. (1994) Cystic fibrosis-type mutational analysis in the ATP-binding cassette transporter signature of human P-glycoprotein MDR1, *J. Biol. Chem. 269*, 20575−83.
61. Bakos, E., Klein, I., Welker, E., Szabo, K., Muller, M., Sarkadi, B., and Varadi, A. (1997) Characterization of the human multidrug resistance protein containing mutations in the ATP-binding cassette signature region, *Biochem. J. 323*, 777−83.
62. Szakacs, G., Ozvegy, C., Bakos, E., Sarkadi, B., and Varadi, A. (2001) Role of glycine-534 and glycine-1179 of human multidrug resistance protein (MDR1) in drug-mediated control of ATP hydrolysis, *Biochem. J. 356*, 71−5.
63. Tombline, G., Bartholomew, L., Gimi, K., Tyndall, G. A., and Senior, A. E. (2004) Synergy between conserved ABC signature Ser residues in P-glycoprotein catalysis, *J. Biol. Chem. 279*, 5363−73.
64. Jones, T. A., Zou, J. Y., Cowan, S. W., and Kjeldgaard, M. (1991) Improved methods for building protein models in electron density maps and the location of errors in these models, *Acta Crystallogr. A47*, 110−9.
65. Zaitseva, J., Jenewein, S., Jumpertz, T., Holland, I. B., and Schmitt, L. (2005) H662 is the linchpin of ATP hydrolysis in the nucleotide-binding domain of the ABC transporter HlyB, *EMBO J. 24*, 1901−10.
66. Sauna, Z. E., Smith, M. M., Muller, M., Kerr, K. M., and Ambudkar, S. V. (2001) The mechanism of action of multidrug-resistance-linked P-glycoprotein, *J. Bioenerg. Biomembr. 33*, 481−91.

BI060308O